COUPLED POLEWARD PROPAGATION OF SEA SURFACE TEMPERATURE AND ATMOSPHERIC ANGULAR MOMENTUM ANOMALIES: RESULTS FROM AMIP

Steven L. Marcus and Jean O. Dickey

Jet Propulsion Laboratory, California Institute of Technology
Pasadena, California

1. INTRODUCTION

In an earlier study incorporating zonally and vertically ave. raged data for the period 1976-1991, Dickey *et al.* (1992- henceforth DMH) found evidence for globally coherent poleward propagation of interannual fluctuations in atmospheric angular momentum (AAM), associated with the El Niño/Southern Oscillation (ENSO) cycle. The bimodality of the. ENSO phenomenon (Rasmusson *et al.*, 1990; Keppenne and Ghil, 1992 and DMH) was evident in spectra of the Southern Oscillation Index and length-of-day (used as a proxy for global AAM variations) during the period of that study, with significant peaks occurring in the low-frequency (LF: 32-88 month) and quasi-biennial (QB: 18-35 month) bands defined by Barnett (1991). Each band was characterized by a distinct AAM teleconnection pattern, with anomalies in the LF band originating near the equator and propagating 10 latitudes greater than 6-0° in both hemispheres, while AAM anomalies in (he. QB band resembled a standing wave in the. tropics, Similar poleward propagation patterns Were found by Yasunari (1987) in the. analysis of 30-60 month filtered zonal wind anomalies; however, the implication of these findings were. not fully pursue.d. Salstein *et al.* (1993a) studied the regional character of this phenomenon using a multi-decade rawinsonde-based data set (Oort, 1983). The purpose of the present study is to investigate the. robustness of this phenomenon by examining interannual AAM variations in an ensemble of nine GCM simulations, performed for the decade 1979.198$ as part of the Atmospheric Model Intercomparison Project (Gates, 1992).

2. DIEZRWTION OF DATA

Fluctuations in atmospheric angular momentum (AAM), a three-dimensional vector, can be divided into two parts: the. changes in the net atmospheric rotation rate, the wind term H^W, and change.s in the net atmospheric moment of inertia, the. pressure term H^P, which arc decoupled to first order. Here, WC. focus on the. third (axial) component, which induces drtec.table length-of-day variations associated with the ENSO cycle, and study the dominant wind term effect by evaluation of:

$$H_3^W = \frac{2\pi R^3}{g}\int\int [u]\ \cos^2\phi\ d\phi\, dp$$

v.'hcrc R is the. mean radius of the Earth, g the acceleration due. to gravity, ϕ the latitude, p the (hydrostatic) pressure, and [u] represents the. ~.onal-mean zonal wind.

Monthly mean value.s of [u] arc. utilized from nine GCM simulations for the period 1979-1988, performed under the auspice.s of the AMIP Program (Gate.s, 1992). Values were provided on two-dimensional latitude-pressure grids, with *resolution* being model dependent. For consistency, the, simulated AAh4 was integrated for all runs from the surface. to 100 mb, the. highest level common to the nine mode.fs considered. For comparison with observations, AAh4 value.s derive.d from U.S. National Meteorological Center (NMC) data were used, based on zonal winds integrated from the surface up to the 100 mb pressure level in 46 equal-arc.a latitude belts (Salstein *et al.*, 19931)). To ensure adequate sampling of the various latitude grids used in the. AMIP runs, all AAM data sets in this study were re-binned into 23 c.qual-area latitude belts, so that the narrowest belt (straddling the equator) has a latitudinal extent of about 5°.

3. ANALYSIS

DMH studied interannual variations in zonally and vertically average.d AAM data from the NMC analysis for the period 1976-1991. The clearest pattern of poleward propagation (see Fig. 1 for the updated version) was found to emerge by applying a simple one-year minus five-year running-mean filter to the

Correspond" author address: Steven L. Marcus, M. *S. 238-332,* Jet Propulsion Laboratory, California Institute of Technology, 4800 Oak Grove Drive, Pasadena, CA 91109.

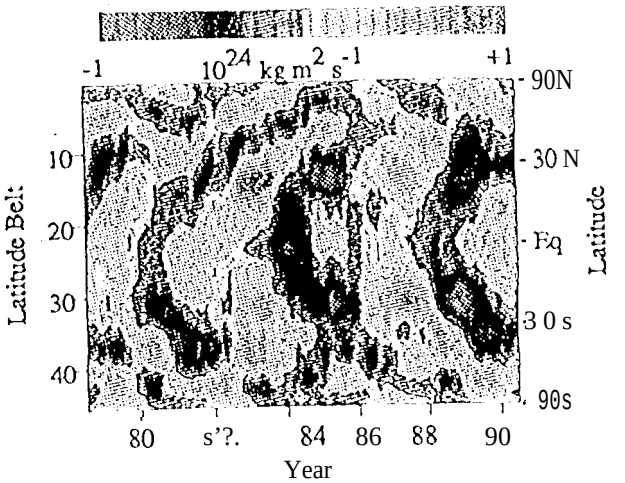

Fig. 1. Onc.-ycar minus five.-ycar moving averages of NMC AAM data in 46 equal-area latitude belts,

AAM in each of the 46 latitude belts, which served to efficiently remove the annual cycle. as well as "decadal" variations from the data. Three complete cycles Of poleward-propagating AAM anomalies arc. visible, with alternating westerlies and easterlies (note the missing data on either end of the. record due to the window c,ffc.et). The shortness of the AMIP records precludes the usc of running averages or Fourier filters to study fluctuations on the. ENSO time scale.. Instead, wc usc the recursive filter described by Murakami (1979), centered at the. period for which the transfer function of the onc.-ycar minus five-year run running mca n filter is largest (44 months). The shortest period (36 months) is chose. n to focus on the poleward-propagating LF variability and to exclude the QB hand, and the longest period (56 months) to make. the. frequency span of the filter symmetric about the maximum.

Fig. 2a shows a Hovmoller diagram formed by filtering monthly values of the NMC AAM data in 23 c.qual-area latitude belts in the 36-56 month band. During the AMIP decade. two complete cycles (easterly and westerly) of poleward-propagagting AAM are visible. The maximum amplitude occurs in the sub-tropics, with the strongest westerly anomalies in both hemispheres coinciding with the. mature phase-s of the 1982-83 and 1986-87 ENSO events. Smaller westerly maxima arc also visible along the equator, preceding the onset of the ENSO episode.s by about one year.

The parallel Hovmoller diagram constructed by filtering the consensus simulation, formed by averaging the rc.suits of the 9 AMIP runs considered, is shown in Fig. 2b. Clearly the model runs capture the poleward propagation of interannual AAM anomalies discussed above, although the propagation speed tends to be somewhat more rapid than observed, especially in the, subtropics of both hemispheres, where. a pattern resembling standing waves is seen. As found in the. observations, westerly anomalies begin at the equator approximately a year before the. onset of the 1982-83 and 1986-87 ENSO events, and intensify as they propsgate polewa rds. Maximum westerly anomalies arc found in the subtropics of both hemisphere.s during the mature phases of both ENSOs, with the 1982-83 event having the strongest amplitude. An interesting aspect of this event is the near-symn~c.try of the. simulated AAM response in the NH and SH subtropics, compared to the much stronger westerlies observed in the NH subtropics during the winter of 1982-83 (Figs. 1 and 2a - scc also Rosen *et al.*, 1984 and DMH). Examination of the. output for each model (not show) indicates that the symmetry of the. consensus run is riot present in the individual simulations, but results from averaging of results containing stronger responses in either of the. two hemispheres. Also of interest is the narrow tongue of easterlies appearing at the equator during the mature phases of both simulated ENSOs. While this feature was previously noted in the NMC data by DMH, it is especially pronounced in the. consensus simulation. anti may indicate. an active role for the. atmosphe re in regulating the duration of El Niño episodes.

Poleward propagation of AAM anomalies may also be visualized in a lag-latitude plot of correlations between individual belts (Riseby and Stone, 198 S). Fig. 3a shows the. lag-correlation between 36-56 month filtered values of NMC AAM, in each of ?.3 c.quai-area latitude belts, with the filtered AAM in the equatorial belt. Slow poleward propagation of AAM anomalies is evident, with coherent signals reaching the subtropics Of both hemispheres at a lag of about 1-2 years. The correlation diagram for filtered AAM from the consensus simulation (Fig. 3b) shows a similar lag between equatorial and sub-tropical maxima, although the, transition between these two regimes is more abrupt than found in the. NMC data, with a sustained period of equatorial AAM anomalies preceding a rapid shift of the. anomalies to the subtropics of both hemispheres.

Correlation coefficients were also computed between filtered AAh4 value.s in neighboring latitude belts for both the NMC data and the consensus simulation, Fig. 4 shows the lag of the poleward belt in each pair for which the correlation coefficient was maximized (the equatorial belt was paired with itself). The consensus results arc. roughly symmetric with respect to the equator, with maxima of polewa rd propagation velocity found in the subtropics (near 10°) and in the. extratropics (near 40°) of both hemispheres. Tropical and subtropical maxima in propagation speed arc also seen in the h^{T}MC data, with all phase velocities being poleward except for the SH extratropics, where the sparseness of observed data renders the analysis less certain.

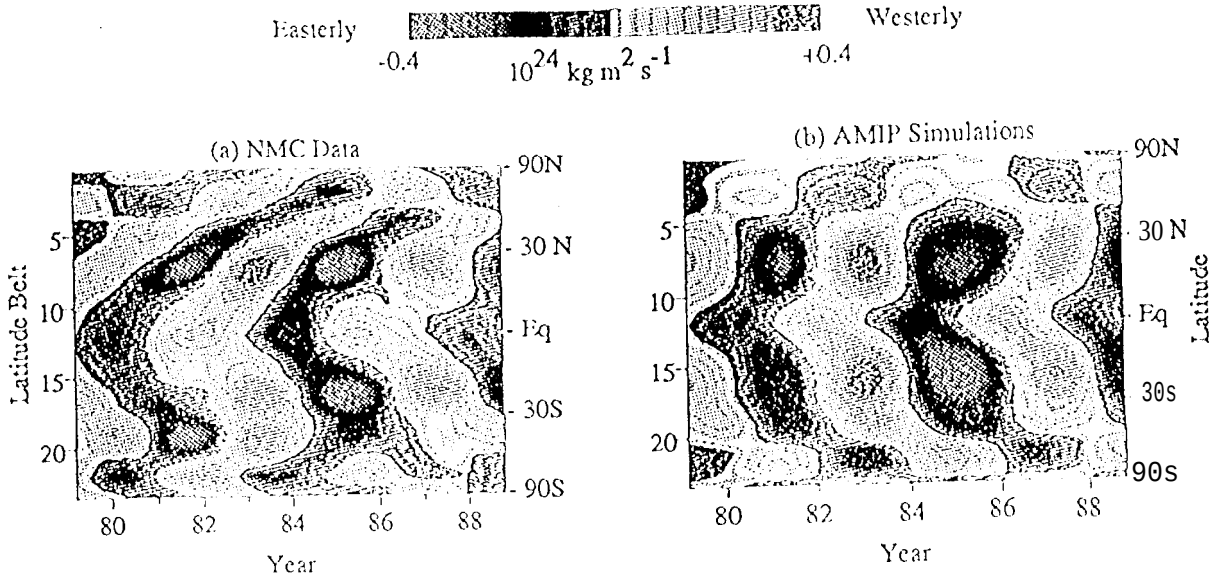

Fig. 2. (a) Hovmoller diagram formed by filtering NMC AAM in the 36-56 month band in 23 equal-area latitude belts. (b) as in (a), for the average of 9 simulations performed as part of the AMIP project.

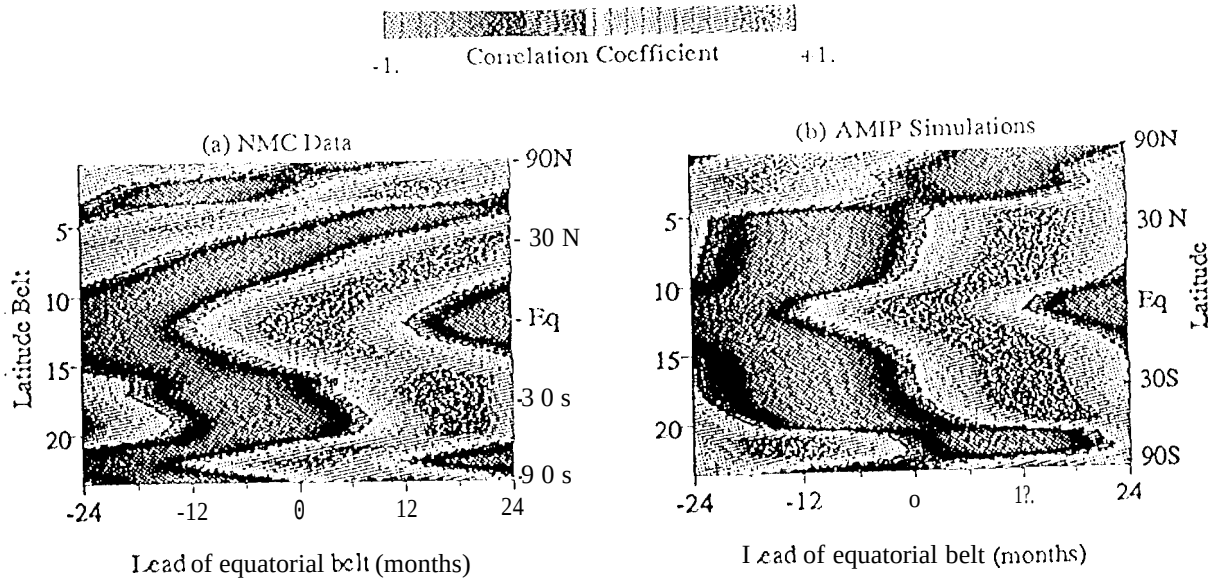

Fig. 3. (a) Lag-correlation of NMC AAM data, filtered in the 36-56 month band in 23 equal-area latitude belts, with the filtered data in the equatorial belt. (b) as in (a), for the average of 9 simulations performed as part of the AMIP project.

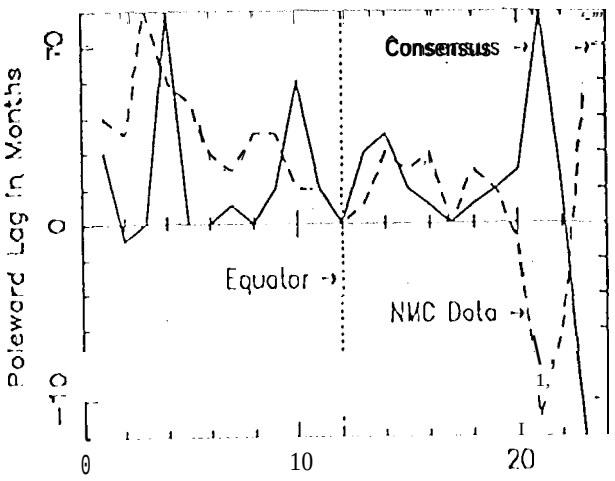

Fig. 4. Solid line: The lag in months for which the correlation coefficient between the 36-56 month filtered AAM in each belt of the. consensus run was maximized with the filtered AAM in the neighboring equatorward belt. Dashed line: as for the solid line, for the NMC AAM data.

in order to assess the robustness of these results, lag-correlation statistics were examined for filtered AAM fluctuations in neighboring latitude belts for all nine. of the model runs. Fig. 5 shows the. number of models which were characterized by standing waves (i.e. maximum correlation at zero lag) or poleward propagation at each latitude. All nine of the. models examined showed poleward or standing propagation for belts 8-16 inclusive (corresponding to latitudes 20°N -- 20°S), indicating the robustness of poleward AAM propagation in the tropics. For the NH extratropics the results fluctuate about the number expected for no directional preference, so that poleward propagation of AAM in this region cannot be inferred from the preliminary AMIP result.. examined here. (On average about one model showed maximum correlation at zero lag for each pair of belts; if there were no directional preference for the AAM propagation, 4 of the. remaining 8 models for each pair of belts would show poleward propagation, so that the expected number with standing or poleward propagation is about 5). For the SH extratropics, on the other hand, the number of models showing poleward or stationary propagation is greater than expected everywhere except for the last pair of bolts, indicating a strong tendency for the simulated AAM, at least, to propagate polewards on interannual time scales.

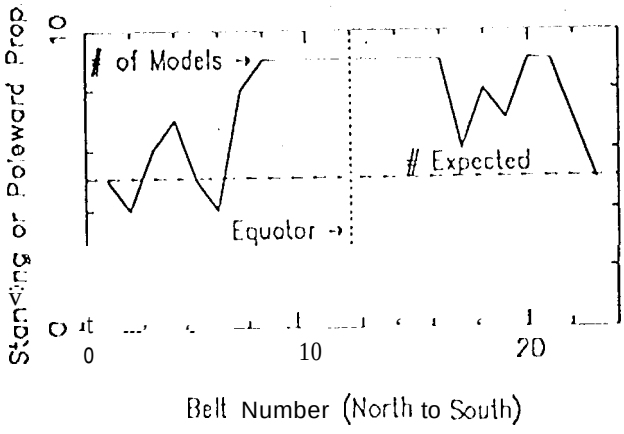

Fig. 5. The number of models (out of a total of 9) showing zero or positive lag in each latitude belt for the. maximum correlation of 36-56 month AAM fluctuations with the neighboring equatorward belt (the equatorial belt was paired with itself). If no directional preference exists, the expected number is 5.07 (see text).

4. DISCUSSION

Since atmospheric dissipation times are generally on the order of a month or less, it is reasonable to expect that the. "memory" of the system for coherent interannual fluctuations lies elsewhere. The most natural candidate. for ENSO-related variability is the ocean, with the sea-surface. temperature (SST) field acting to communicate. the oceanic state to the

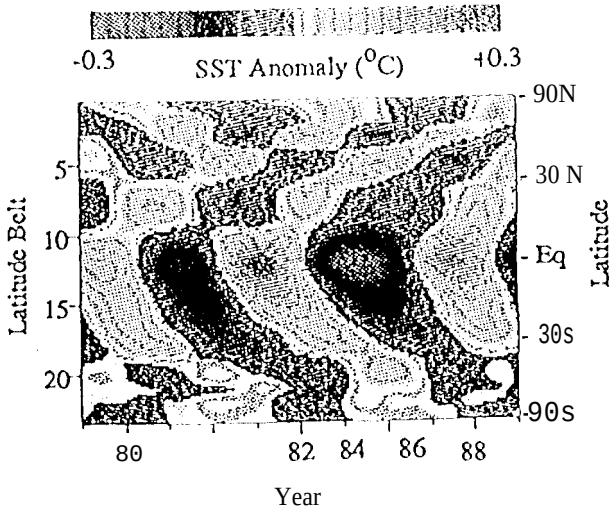

Fig. 6. Hovmoller diagram formed by filtering the zonal mean of the SST data used as boundary conditions for the AMIP runs in the 36-56 month band, in 23 equal-area latitude belts.

atmosphere'. Since AAM is a zonally-averaged quantity, we present in Fig. 6 a Hovmoller diagram of the Z.onally-averaged SST data, filtered in the 36-56 month band, which was used to drive the AMIP simulations described above. A pattern of pole.ward propagation clearly exists, with phase speeds similar to that found in the, NMC data (Fig. 2a). Whereas the observed AAM propagation has the largest range in the NH, however, the SST propagation appears more robust in the SH, which has more ocean-covered surface. The consensus AAM simulation also shows the greatest range of propagation in the SH, although the. speed of the propagation differs considerably from that found in both the observed AAM and SST fields. Further studies will be needed to determine. the extent to which these atmospheric phenomena result from oceanic. forcing, and the mechanism by which this forcing generates the globally-propagating AAM anomalies documented in this and previous studies.

Acknowledgments. The AMIP Diagnostic Subproject on AAhl is headed by R. Hide and also include R. D. Rosen and D. A. Salstein. The authors thank David A. Salstein for supplying the. banded NMC AAM data used in our analysis. 'l-he work described in this paper was carried out at the Jet Propulsion Laboratory, California Institute of Technology, under contract with the National Aeronautics and Space Administration.

REFERENCES

Barnett, T. P., 1991: The interaction of multiple time scales in the tropical climate system, *J. Climate*, 4, 269-285.

Dickey, J. O., S. L. Marcus and R. Hide, 1992: Glottal propagation of interannual fluctuations in atmospheric angular momentum, *Nature*, 3s7, 482-488.

Gate.s, W. 1.., 1992: AMIP: The Atmospheric Model Intercompa risen Project, *Bull. Amer. Meteor. Sot.*, 73, 1962-1970.

Keppenne, C. 1.., and M. Ghil, 1992: Adaptive filtering and prediction of the Southern Oscillation Index, *J. Geophys. Res.*, 97, 20,449-20,454.

Murakami, M., 1979: I.arge-scale aspects of deep convective activity over the GATE area, *Mon. Weather Rev.*, 107, 994-1013.

Oort, A. H., 1983: Global atmospheric circulation statistics, 1958-1973, U. S. Dept. of Commerce, *NOAA Professional Paper 14.*

Rasmusson, E. M., X. Wang, and C. F. Ropelewski, 1990: The biennia] component of ENSO variability, *J. Mar. Systems*, *1*, 71-96.

Riseby, J. S., and P. H. Stone, 1988: Observations of the 30-60 day oscillation in renal mean atmospheric angular momentum and high cloud cover, *J. Atmos. Sci.*, **45**, *2026-2038.*

Rosen, R. D., D. A. Salstein, T. M. Eubanks, J. O. Dickey, and J. A. Steppe., 1984: An El Niño signal in atmospheric angular momentum and Earth rotation, *Science*, 22S, 411-414.

Salstein, D. A., R. X, Black and R. D. Rosen, 1993a: Interannual variations in angular momentum from a rawinsondc-base.d climate data set, Fourth Symposium on Global Change Studies (held January 17-22, 1993; Anaheim, California), 331-334, *American Meteorological Society*, Boston.

Salstein, D. A., D. M. Kann, A. J. Miller, and R. D. Rosen, 1993b: The Sub-Bureau for Atmospheric Angular Momentum of the International Earth Rotation Service: A meteorological data center with geodetic applications, *Bull. Amer. Meteor. Sot.*, 74, 67-80.

Yasunari, "1'., 1987: Global structure of the El Nifio/Southern Oscillation: Part II. time evolution, *J. Meteorol. Sot. Japan*, 65, 81-102.